ISSN (Online) 2395-2717
International Journal of Engineering Research in Electrical and Electronic Engineering (IJEREEE)
Vol 2, Issue 8, August 2016

Model Predictive Control of Three-Phase Four Switch Inverter-Fed Induction Motor Drives

[1] Pala Prasad Reddy M, [2] Harinath Reddy K [3] Swathi S
[1][2][3]Assistant Professor [3]M.Tech (Electrical Power Engineering)
Department of EEE,
Annamacharya Institute of Technology and Sciences, Rajampet-516126

Abstract: **-- The four-switch three-phase (B4) inverter has the possibility of reducing the inverter cost, and it became very attractive in fault-tolerant control to solve the open/short-circuit faults of the six-switch three-phase (B6) inverter. Its application is limited due to the fluctuation of the two dc-link capacitor voltages which causes the unbalance among the phase currents. Predictive torque control (PTC) scheme is proposed for the B4 inverter-fed induction motor (IM) with the dc-link voltage offset suppression. For precise prediction and control of the torque and stator flux, the voltage vectors of the B4 inverter under the fluctuation of the two dc-link capacitor voltages are derived. By directly controlling the stator flux, the three-phase currents are forced to stay balance. The voltage offset of the two dc-link capacitors is modeled and controlled in the predictive point of view.**

Keywords**: Model Predictive Control(MPC), Induction Motor(IM), four switch inverter, cost function, current unbalance.**

I. INTRODUCTION

Over the years, the conventional three-phase voltage source inverter with six switches (B6) has been found widespread industrial applications in various forms, such as motor drives and active filters. However, in certain applications, a further cost reduction for inverter configuration is considered by users. To achieve this goal, the three-phase inverter with only four switches was proposed by Van der Broeck and Van Wyk [1] for the purpose of minimizing the components' cost, and it is named four-switch three-phase (B4) inverter in comparison with the B6 one, as shown in Fig. 1. Although this kind of cost reduction is at the expense of output performance, the B4 inverter can be utilized in fault-tolerant control to solve the open/short-circuit fault of the B6 inverter. The idea of the B4 inverter applied to fault-tolerant control is very valuable in some critical occasions such as rail traction, and it has consequently attracted the interest of many researchers [2],[3].

The four-switch inverters are known to have several disadvantages compared to normal six-switch inverters: the voltage utilization factor is halved compared to the six-switch inverter. On the other hand, the capacitor center tap voltage is fluctuating, and it destroys the balance among the motor phase currents [4]. The capacitor center tap voltage fluctuation increases as the load torque becomes higher or the frequency of a B4 inverter becomes lower, and the unbalanced motor current leads to an inverter failure and torque pulsation.

In order to mitigate the effects of the capacitor center tap voltage fluctuation, several papers were published [5],[6]. With the development of fast and powerful microprocessors, increasing attention has been dedicated to the use of model predictive control (MPC) in power electronics [7]. The first ideas about this strategy applied to power converters started in the 1980s [8], [9].

The main concept is based on calculating the system's future behaviour to obtain optimal values for the actuating variables. With this intuitive concept, predictive control can be applied to a variety of systems, in which constraints and nonlinearities can be easily included, multivariable case can be considered, and the resulting controller is easy to implement. In the PTC, the complete model and future behaviour of the inverter-fed drives are taken into account. A cost function relating to torque and flux errors reduction is defined to evaluate the effects of each voltage vector and the one minimizing the cost function is selected [10],[11]. In spite of the outstanding performance of B6 inverter-fed drives based on the PTC, PTC for B4 inverter-fed drives did not get many attentions to the researchers. Some simulation results of PTC for the B4 inverter-fed drives emulating the B6 case were carried out in [11]. However, the dc-link voltages fluctuation, which is the intrinsic feature of the B4 inverter, was not considered.

Additionally, and the offset suppression of the two capacitor voltages was not mentioned.

ISSN (Online) 2395-2717
International Journal of Engineering Research in Electrical and Electronic Engineering (IJEREEE)
Vol 2, Issue 8, August 2016

In this paper, the special issues on using the famous PTC control scheme for B4 inverter-fed IM drives are analyzed and discussed. Because of the halved switch states corresponding to B6 one, the real-time implementation time cost for the PTC scheme in B4 inverter is reduced in a sampling period.

II. B4 INVERTER AND IM MODELING

A. Intrinsic Voltage Vector of a B4 Inverter

Fig.1 shows the B4 topology having a two leg inverter in which switches(T1 – T4) are considered ideal (i.e., no saturation voltage drop and no dead time) for our convenient analysis. S_b and S_c can be used as binary state variables to denote the switching states of leg b (T1,T2) and leg c (T3,T4) respectively. The dc-link is split in to two voltage sources, one load phase is connected to the middle of dc-link. The simultaneous closed states of two switches in each leg is usually avoidable inorder to prevent the short circuit of dc-link. Therefore, binaries 1 and 0 will indicate the closed states of upper switch and lower switch respectively. By assuming the three-phase voltages as balanced, the phase-to-neutral voltages V_{aN} ,V_{bN} ,V_{cN} are as follows:

$$V_{aN} = \frac{V_{dc1}}{3}(-S_b - S_c) + \frac{V_{dc2}}{3}(2 - S_b - S_c)$$

$$V_{bN} = \frac{V_{dc1}}{3}(2 - S_b - S_c) + \frac{V_{dc2}}{3}(2 - S_b - S_c - 1)$$

$$V_{cN} = \frac{V_{dc1}}{3}(2 - S_c - S_b) + \frac{V_{dc2}}{3}(2 - S_c - S_b - 1) \quad (1)$$

Where V_{dc1} and V_{dc2} are the upper and the lower dc-link capacitor voltages, respectively

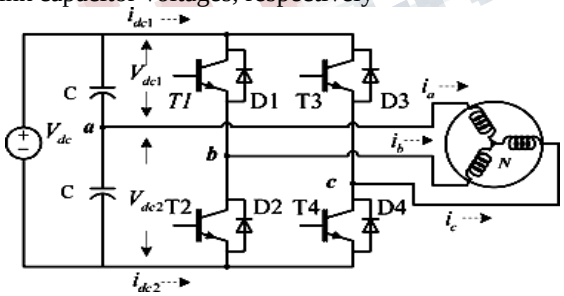

Fig.1: Circuit diagram of B4 inverter-fed Induction motor drive

Table I gives the phase-to- neutral voltages values by considering all the possible combinations of (S_b ,S_c).

The Clarke transform applied to the stator voltages yields as follows:

$$\begin{bmatrix} V_{\alpha s} \\ V_{\beta s} \end{bmatrix} = \frac{2}{3}\begin{bmatrix} 1 & -\frac{1}{2} & -\frac{1}{2} \\ 0 & \frac{\sqrt{3}}{2} & -\frac{\sqrt{3}}{2} \end{bmatrix}\begin{bmatrix} V_{aN} \\ V_{bN} \\ V_{cN} \end{bmatrix} \quad (2)$$

where the $V_{\alpha s}$ and $V_{\beta s}$ are the α- and β-axis stator voltage, respectively. The voltage vectors are expressed by $\overrightarrow{v_s} = V_\alpha + jV_\beta$.

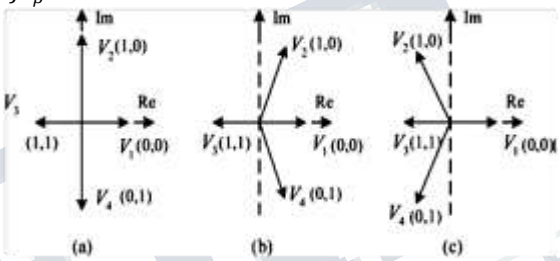

Fig.2: Basic voltage vectors of theB4 inverter(a) V_{dc1} =V_{dc2}

(b) $V_{dc1} < V_{dc2}$ and (c) $V_{dc1} > V_{dc2}$

It can be seen clearly that in Table II which gives the four active voltage vectors(V1-V4) in the $\alpha\beta$ plane, the B4 inverter can only produce four basic nonzero voltage vectors.

Table 1: B4 Inverter Switching Functions and Output Voltages

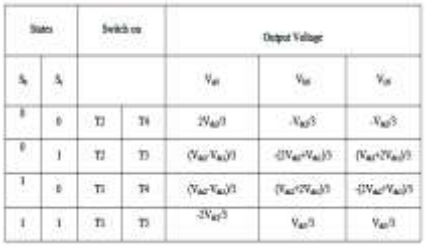

Fig.2(a) represents the four voltage vectors when the values of the upper and lower capacitance are big enough to keep the capacitor voltages a constant value of $V_{dc}/2$. Fig.2(b) and (c) presents the vector positions in the conditions of $V_{dc1} < V_{dc2}$ and $V_{dc1} > V_{dc2}$ respectively.

ISSN (Online) 2395-2717
International Journal of Engineering Research in Electrical and Electronic Engineering (IJEREEE)
Vol 2, Issue 8, August 2016

Table II: Basic Voltage vectors of the B4 Inverter

Switching states (S_b, S_a)	Voltage Vectors ($\overrightarrow{v_s}$)	Vector Symbol
00	$2V_{dc}/3$	V1
10	$(V_{dc}-V_{dc})/3-j\sqrt{3}((V_{dc}+V_{dc})/3$	V2
11	$(V_{dc}-V_{dc})/3+j\sqrt{3}((V_{dc}+V_{dc})/3$	V3
01	$-2V_{dc}/3$	V4

B. Machine Equations

Stator variables, voltage $\overrightarrow{v_s}$, current $\overrightarrow{i_s}$, and flux $\overrightarrow{\varphi_s}$ are electrically related according to

$$\overrightarrow{v_s} = R_s\overrightarrow{i_s} + \frac{d\overrightarrow{\varphi_s}}{dt} \quad (3)$$

where *Rs* is the stator resistance.
Rotor equation in a stator reference frame represents the relation between rotor current $\overrightarrow{i_r}$ and rotor flux $\overrightarrow{\varphi_r}$ as follow

$$0 = R_r\overrightarrow{i_r} + \frac{d\overrightarrow{\varphi_r}}{dt} - j\omega\overrightarrow{\varphi_r} \quad (4)$$

where *Rr* is the rotor resistance and ω is the rotor speed.

Flux linkage equations relate stator and rotor currents are given in (5) and (6), where L_m, L_s and L_r are the mutual, stator, and rotor inductances, respectively

$$\overrightarrow{\varphi_s} = L_s\overrightarrow{i_s} + L_m\overrightarrow{i_r} \quad (5)$$

$$\overrightarrow{\varphi_r} = L_m\overrightarrow{i_s} + L_r\overrightarrow{i_r} \quad (6)$$

Electromagnetic torque *Te* can be expressed in terms of stator current and stator flux

$$T_s = \frac{3}{2}p\overrightarrow{\varphi_s} \times \overrightarrow{i_s} \quad (7)$$

where *p* is the number of pole pairs.
The ratio of change in the mechanical rotor speed ω by the Torque

$$J\frac{d\omega}{dt} = T_e - T_L \quad (8)$$

where the coefficient *J* denotes the moment of inertia of the mechanical shaft, and T_L is the load torque to the machine.

III. ALGORITHM FOR THE PTC SCHEME

A three-step algorithm is carried out in any standard PTC scheme: flux estimation, flux and torque prediction, and cost function optimization, [10]. The structure of the B4 inverter-fed IM drive-based PTC scheme is shown in Fig. 3 in which the inner loop is a stator flux and electromagnetic torque controller based on PTC, while the outer speed loop is a traditional PI controller.

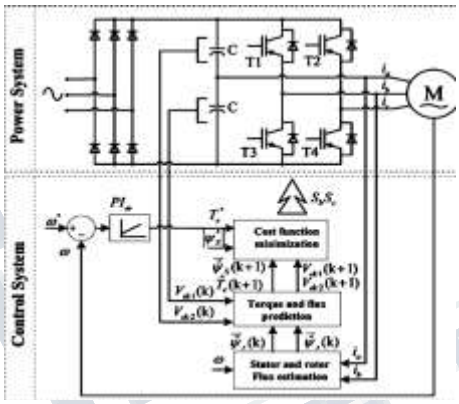

Fig.3: Structure of the B4 inverter-fed IM drive based on the PTC scheme.

A. Flux Estimation

The dc-link voltage ripple existence in the B6 inverter means a proportional alteration of all three output phase voltages and accordingly an amplitude error of the average voltage vector used. Whereas in a B4 inverter, the voltage ripple leads to different modification of the voltages on the three phase (see Table I) and to both amplitude and angular errors of the switching voltage vectors. Moreover, a significant fluctuation of the dc-link voltages is inevitable due to one-phase current flows through the split dc-link voltage sources. Hence, the voltage-model-based flux estimator using the command voltages becomes less accurate in the B4 case whereas in the B6case, it can approximately estimate the stator flux [10].

Current-model-based flux estimator using instant currents and speed signals are adopted in the proposed scheme and at the present sampling step *k* the estimations of the stator flux $\overrightarrow{\varphi_s}$ and the rotor flux $\overrightarrow{\varphi_r}$ are required. The rotor flux can be calculated using equivalent equation of an induction machine.

ISSN (Online) 2395-2717
International Journal of Engineering Research in Electrical and Electronic Engineering (IJEREEE)
Vol 2, Issue 8, August 2016

$$\overrightarrow{\varphi_r} + \tau_r \frac{d\overrightarrow{\varphi_r}}{dt} = -j\tau_r(\omega_k - \omega)\overrightarrow{\varphi_r} + L_m\overrightarrow{i_s} \quad (9)$$

where $\tau_r = \frac{L_r}{R_r}$, $\boldsymbol{\omega}_k$ the angular speed of a rotating coordinate frame, and ω corresponds to the rotor speed. Writing (9) in terms of a rotating reference frame aligned with the stator winding ($\boldsymbol{\omega}_k = 0$) is given as follows:

$$\overrightarrow{\varphi_r} + \tau_r \frac{d\overrightarrow{\varphi_r}}{dt} = L_m\overrightarrow{i_s} + j\omega T_r\overrightarrow{\varphi_r} \quad (10)$$

For the stator flux estimation, the rotor linkage (6) is used to write the rotor current in terms of the measured stator currents and the estimated rotor flux. Then, by replacing $\overrightarrow{i_r}$ of (6) in the stator flux (5), the stator flux estimation is obtained

$$\overrightarrow{\varphi_s} = L_m\left(\frac{\overrightarrow{\varphi_r} - L_m\overrightarrow{i_s}}{L_r}\right) + L_r\overrightarrow{i_r} \quad (11)$$

Using Euler-based discretization in (10) and (11), the discrete equations of the rotor and stator flux estimation are as follows:

$$\overrightarrow{\widehat{\varphi_r}}(k) = \frac{T_r}{T_s(1-j\omega T_r)}\overrightarrow{\varphi_r}(k-1) + \frac{L_m}{1-j\omega T_r}\overrightarrow{i_s}(k) \quad (12)$$

$$\overrightarrow{\widehat{\varphi_s}}(k) = k_r\overrightarrow{\widehat{\varphi_r}}(k) + \sigma L_s\overrightarrow{i_s}(k) \quad (13)$$

Where T_s corresponds to the sampling time, $K_r = L_m / L_r$ is the rotor coupling factor and $\sigma = 1 - (\frac{L_m^2}{L_m L_s})$ is the total leakage factor.

The rotor flux estimation is obtained without using the command voltages in (12). Thus, the accurate flux estimation for the B4 inverter-fed IM is achieved.

B. Stator Flux and Electromagnetic Torque Prediction

Stator flux and electromagnetic torque are the control variables, so that their behaviours must be predicted at sampling step $k + 1$.

The stator flux prediction $\overrightarrow{\widehat{\varphi_s}}(k+1)$ is obtained by the stator voltage equation.

Using the Euler formula to discretize (3) and shifting the result to a single time step, the stator flux prediction is obtained

$$\overrightarrow{\widehat{\varphi_s}}(k+1) = \overrightarrow{\widehat{\varphi_s}}(k) + T_s\overrightarrow{v_s}(k) - R_sT_s\overrightarrow{i_s}(k) \quad (14)$$

where *Ts* is the sampling time used in the PTC algorithm.

The electromagnetic torque prediction can be calculated as

$$\widehat{T_e}(k+1) = \frac{3}{2}p \cdot Im\{\overrightarrow{\widehat{\varphi_s}}(k+1) \cdot \overrightarrow{i_s}(k+1)\} \quad (15)$$

The prediction expression of the stator current $\overrightarrow{i_s}(k+1)$ is obtained using the equivalent equation of the stator dynamics of an induction machine

$$\overrightarrow{v_s} = R_s\overrightarrow{i_s} + L_\sigma\frac{d\overrightarrow{\varphi_s}}{dt} - k_r(\frac{1}{T_r} - j\omega)\overrightarrow{\varphi_r} \quad (16)$$

where $R_\sigma = R_s + K_r^2R_r$ corresponds to the equivalent resistance and $L_\sigma = \sigma L_s$ is the leakage inductance of the machine.
The last term in (16) represents the cross coupling between the rotor and the stator winding through the induced voltage. Thus, replacing the derivatives with the Euler formula in (16), the prediction equation of the stator current $\overrightarrow{i_s}$at the instant $k + 1$ is obtained .

(12)

$$\overrightarrow{i_s}(k+1) = \left(1 + + \frac{T_s}{\tau_\sigma}\right)\overrightarrow{i_s}(k) + \frac{T_s}{\tau_\sigma + T_s}\{\frac{1}{R_\sigma}\left(\left(\frac{k_r}{\tau_r} - j\omega k_r\varphi_{rk} + v_{sk}\right)\right. \quad (13)$$

(17)

Once the predictions of the stator flux (14) and the stator current (17) are obtained, the prediction of the electromagnetic torque can be calculated in (15).

C. Cost Function Optimization

The next step in predictive control is the optimization of an appropriate control law that is defined as a cost function. The structure form of the cost function is given as follows:

$$g_i = \frac{\left|T_e^* - \widehat{T_e}(k+1)_i\right|}{T_{e_{nom}}} + \lambda_0\frac{\left|\left\|\overrightarrow{\varphi_s^*}\right\| - \left\|\overrightarrow{\widehat{\varphi_s}}(k+1)_i\right\|\right|}{\left\|\overrightarrow{\varphi_s}\right\|_{nom}}$$

$i \in \{1,2,3,4\}$ (18)

ISSN (Online) 2395-2717
International Journal of Engineering Research in Electrical and Electronic Engineering (IJEREEE)
Vol 2, Issue 8, August 2016

where *i* denotes the index of the stator voltage vector used to calculate the predictions $\widehat{T_e}(k+1)$ and $\widehat{\varphi_s}(k+1)$, respectively.

The rated torque $T_{e_{nom}}$ and the rated stator flux magnitude $\|\overrightarrow{\varphi_s}\|_{nom}$ are used to normalize the cost function terms. The torque reference is externally generated by a PI speed controller. The factor λ_0 denotes a weight factor. Finally, the optimization step is carried out, and the inverter voltage vector that minimizes the cost function is selected as the optimal switching state for the next sampling period *k* + 1, thus the optimal torque and flux control is achieved.

D. Time-Delay Compensation

It is well known that there is one-step delay in digital implementation. In other word, the voltage vector selected at the instant time k will not be applied until the instant time *k* + 1 [10]. To eliminate this delay, the value at the instant time *k* + 2 should be used in (18) rather than the instant time *k* + 1. Therefore, the cost function (18) is redefined as

$$g_i = \frac{\left|T_e^* - \widehat{T_e}(k+2)_i\right|}{T_{e_{nom}}} + \lambda_0 \frac{\left|\|\overrightarrow{\varphi_s^*}\| - \|\overrightarrow{\widehat{\varphi_s}}(k+2)_i\|\right|}{\|\overrightarrow{\varphi_s}\|_{nom}}$$

$i \in \{1,2,3,4\}$ (19)

E. DC-Link Voltage Offset Suppression

The inappropriate initial phase angle of phase "a" current or the imbalance current flowing in the two capacitors will cause voltage deviation [5]. Therefore, suppressing the offset of the two capacitor voltages is necessary.

$$g_i = \frac{\left|T_e^* - \widehat{T_e}(k+2)_i\right|}{T_{e_{nom}}} + \lambda_0 \frac{\left|\|\overrightarrow{\varphi_s^*}\| - \|\overrightarrow{\widehat{\varphi_s}}(k+2)_i\|\right|}{\|\overrightarrow{\varphi_s}\|_{nom}} + \lambda_{dc} \frac{\left|\widehat{V_{dc1}}(k+1)_i - \widehat{V_{dc2}}(k+2)_i\right|}{V_{dc}}$$

$i \in \{1,2,3,4\}$ (24)

Where $V_{dc}$is dc-link voltage, which can be obtained by $V_{dc}=V_{dc1}+V_{dc2}$, λ_{dc} is the weight factor of the dc-link capacitor voltage offset suppression. By an exhaustive search for all feasible voltage vectors, the minimization of (24) is done. The proposed control scheme can be implemented in the following sequence as shown in Fig.4.
The superscript *k*, *k* + 1, and *k* + 2 denote the variables' value at sampling time *k*, *k* + 1, and *k* + 2, respectively. $\overrightarrow{v_{opt}^k}$ and $\overrightarrow{v_{opt}^{k+1}}$are the optimal voltage vectors found in the previous loop iteration and the current loop iteration, respectively.

As it is shown earlier, a high degree of flexibility is obtained with the proposed control scheme due to the online optimization algorithm, where the system nonlinearities and restrictions (i.e., capacitor voltage offset suppression) can be included in the cost function.

IV. ANALYSIS OF WEIGHTING FACTORS

Weighting factor are the only parameters that are supposed to adjust in the proposed scheme which is clear from (24).

Effect of the weighting factors can be analysed by performing the extensive simulation in MATLAB/Simulation. Table III shows the ratings and parameters of the B4 inverter and IM.

A. Stator Flux Weighting Factor λ_0

Weighting factor(λ_0) increases or decreases the relative importance of the torque versus flux control. λ_0= 1 if the same importance is assigned to both control objectives.

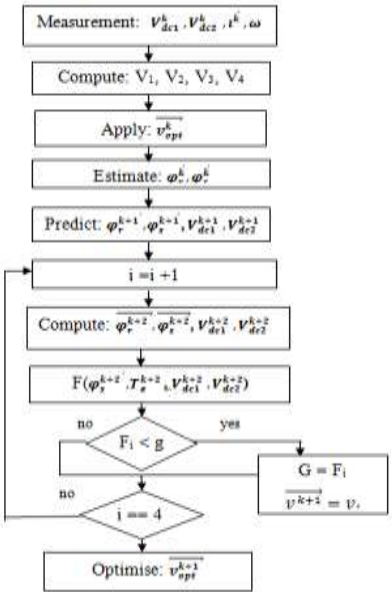

Fig.4: Implementation flowchart of the proposed scheme

ISSN (Online) 2395-2717
International Journal of Engineering Research in Electrical and Electronic Engineering (IJEREEE)
Vol 2, Issue 8, August 2016

A higher weighting factor λ_0 is expected (e.g., λ_0 = 3) to obtain the balanced currents versus the unbalanced structure of B4 inverter. Fig.5 shows the simulation results During a speed-reversal from 500 to –500 r/min at 50% rated load torque for the case of λ_0=3 where the stator flux reference is the nominal one at 0.6Wb. A comparable study for the same system is made with smaller weighting factor, λ_0 = 1 are presented in Fig.6. Here, it can be appreciated that the flux exhibits a higher ripple during steady state when compared to the previous case. During the transient, the balanced three-phase currents collapse due to the failure in stator flux control.

So, considering the good performance, in the remaining tests, the tuning factors λ_0 will be kept at the value of λ_0 = 3.

Table III: Parameters of B4 inverter and IM

PARAMETERS	RATINGS
DC-link voltage	540 V
DC-link upper capacitor (C1)	2040 μF
DC-link upper capacitor (C2)	2040 μF
Dead time	4 μs
Induction Motor	
Rated power	2.2 kW
Rated voltage	380 V
Rated speed	1430 r/min
Rated current	4.9 A
Rated frequency	50 Hz
Number of poles	4
Stator resistance (R_s)	2.804 Ω
Stator leakage inductance (L_s)	10.33 mH
Rotor resistance (R_r)	2.178 Ω
Rotor leakage inductance (L_r)	10.33 mH
Magnetizing inductance (L_m)	319.7 mH
Nominal flux-linkage	0.6 Wb
Rated torque	14 N·m

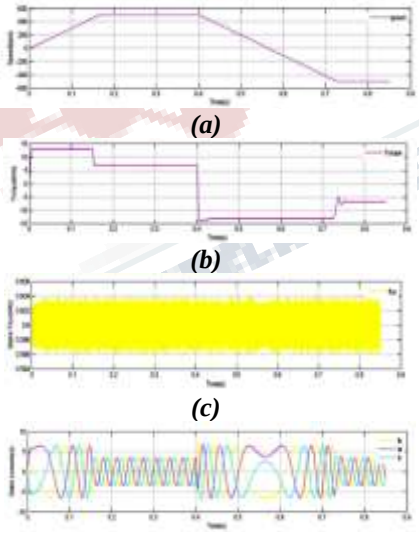

(a)

(b)

(c)

(d)

Fig.5: Simulated waveforms using the PTC scheme for a B4 Inverter for λ_0=3 (a)Speed (b)Torque (c)Stator Flux (d)Stator Currents

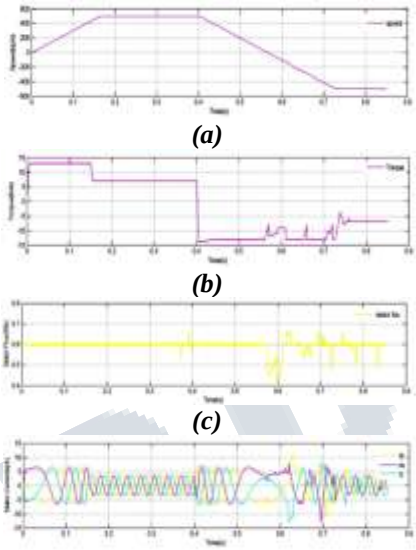

(a)

(b)

(c)

(d)

Fig.6: Simulated waveforms using the PTC scheme for a B4 inverter for λ_0=1 (a)Speed (b)Torque (c)Stator Flux (d)Stator Currents

B. Capacitor Voltages Offset Suppression Weighting Factor λ_{dc}

The weighting factor λ_{dc} increases or decreases the relative importance of the dc-link capacitor voltage offset suppression versus the control performance. With a higher value of the weighting factor λ_{dc}, the two capacitor voltages converge faster, but when a very high value of this weighting factor is applied, the control performance is affected.

The simulation results at the speed of 500 r/min with a torque of 10Nm are shown in Figs. (7) and (8) in case of λ_{dc} =1000 and λ_{dc} = 2000, respectively. In Fig.7, after the voltage offset suppression term is added at t=3s, the two capacitor voltages converge to 270V at t=7s, and as it is shown that a slight increment in the torque ripple occurs when the capacitor voltage offset term is added. This is acceptable with negligible effect on the flux and speed waveforms. For a comparative study, the results in the cases of λ_{dc} =2000 are shown in Fig.8. It can be noticed that the converging time of the two capacitor voltages is approximately 1s, but a significant stator flux and torque ripples are exhibited in the steady state. In consideration of the good performance obtained, in the remaining tests, the tuning factors λ_{dc} will be kept at the value of λ_{dc} = 1000.

ISSN (Online) 2395-2717
International Journal of Engineering Research in Electrical and Electronic Engineering (IJEREEE)
Vol 2, Issue 8, August 2016

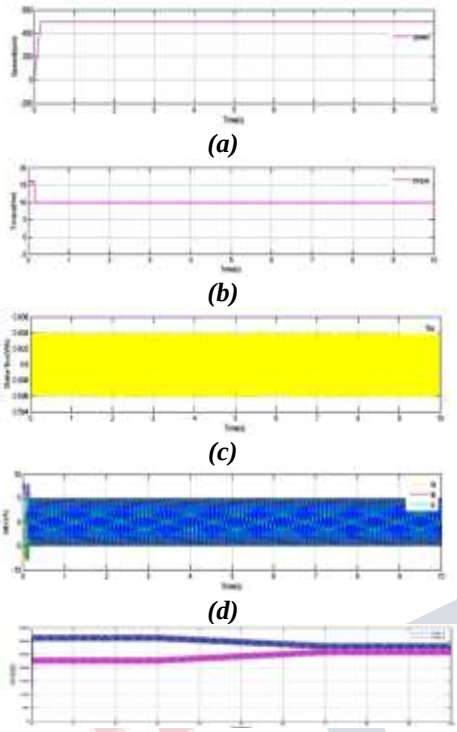

(a)

(b)

(c)

(d)

(e)

Fig.8:Simulated waveforms using the PTC scheme with λ_{dc}=1000 (a)Speed (b)Torque (c)Stator Flux (d)Stator Currents (e)Capacitor Voltages

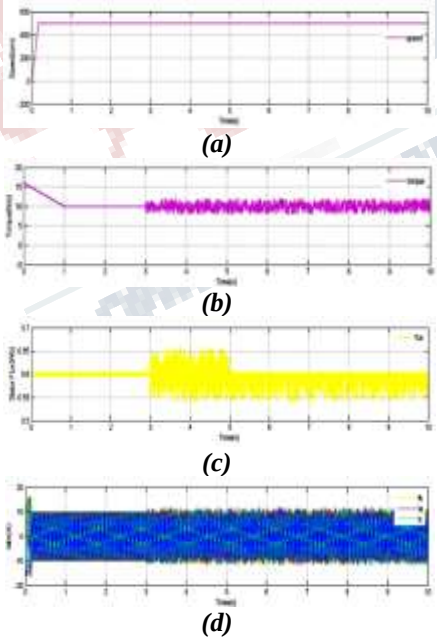

(a)

(b)

(c)

(d)

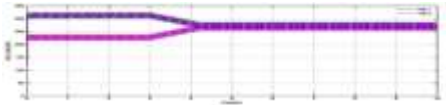

(e)

Fig.9:Simulated waveforms using the PTC scheme with λ_{dc}=2000 (a)Speed (b)Torque (c)Stator Flux (d)Stator Currents (e)Capacitor Voltages

VI. CONCLUSION

The PTC scheme for the B4 inverter fed IM drives is analysed and discussed. For the precise prediction and control of the torque and stator flux, the voltage vectors of the b4 inverter are derived under the fluctuations of the two dc-link capacitor voltages. The investigation is carried out on the design and performance evaluation of the PTC scheme for the B4 inverter fed IM drive and achieved the balanced three-phase currents along with the suppression of capacitor voltage offset. Considering the cost reduction and its advantages, the proposed B4 inverter fed IM drive has been found acceptable for the high performance industrial variable-speed-drive applications. Certainly, the additional work is still remained to develop more efficient PTC scheme when the question of parameter deviation is arised.

REFERENCES

[1]. H. W. Van der Broeck and J. D. Van Wyk, "A comparative investigation of a three-phase induction machine drive with a component minimized voltage-fed inverter under different control options," *IEEE Trans. Ind. Appl.*, vol. IA-20, no. 2, pp. 309–320, Mar. 1984.

[2]. B. A. Welchko, T. A. Lipo, T. M. Jahns, and S. E. Schulz, "Fault tolerant three-phase AC motor drive topologies: A comparison of features, cost, and limitations," *IEEE Trans. Power Electron.*, vol. 19, no. 4, pp. 1108– 1116, Jul. 2004.

[3]. R. L. D. Ribeiro, C. B. Jacobina, E. R. C. da Silva, and A. M. N. Lima, "Fault-tolerant voltage-fed PWMinverter AC motor drive systems," *IEEE Trans. Ind. Electron.*, vol. 51, no. 2, pp. 439–446, Apr. 2004.

[4]. F. Blaabjerg, D. O. Neacsu, and J. K. Pedersen, "Adaptive SVM to compensateDC-Link voltage ripple for four-switch three-phase voltage-source inverters,"

IEEE Trans. Power Electron., vol. 14, no. 4, pp. 743–752, Jul. 1999.

[5]. R. Wang, J. Zhao, and Y. Liu, "A comprehensive investigation of fourswitch three-phase voltage source inverter based on double Fourier integral analysis," *IEEE Trans. Power Electron.*, vol. 26, no. 10, pp. 2774–2787, Oct. 2011.

[6]. B. El Badsi, B. Bouzidi, andA.Masmoudi, "DTCscheme for a four-switch inverter-fed induction motor emulating the six-switch inverter operation," *IEEE Trans. Power Electron.*, vol. 28, no. 7, pp. 3528–3538, Jul. 2013.

[7]. J. H. Lee, "Model predictive control: Review of the three decades of development," *Int J Control Autom.*, vol. 9, no. 3, pp. 415–424, Jun. 2011.

[8]. J. Holtz and S. Stadtfeldt, "A predictive controller for the stator current vector of ac machines fed from a switched voltage source," in *Proc. IEEE IPEC*, 1983, vol. 2, pp. 1665–1675.

[9]. R. Kennel and D. Sch¨oder, "A predictive control strategy for converters," in *Proc. IFAC Control Power Electron. Elect. Drives*, 1983, pp. 415–422.

[10]. J. Rodriguez, R. M. Kennel, J. R. Espinoza, M. Trincado, C. A. Silva, and C. A. Rojas, "High-performance control strategies for electrical drives: An experimental assessment," *IEEE Trans. Ind. Electron.*, vol. 59, no. 2, pp. 812–820, Feb. 2012.

[11]. M.Habibullah and D. D. C. Lu, "Predictive torque and flux control of afour-switch inverter-fed IM drive," in *Proc. 1st Int. Future Energy Electron.Conf.*, 2013, pp. 629–634.